

PHYSICAL REVIEW LETTERS

VOLUME 69

30 NOVEMBER 1992

NUMBER 22

Long-Wavelength Oscillations and the New Gallium Solar Neutrino Signals

V. Barger,⁽¹⁾ R. J. N. Phillips,⁽²⁾ and K. Whisnant⁽³⁾

⁽¹⁾*Physics Department, University of Wisconsin, Madison, Wisconsin 53706*

⁽²⁾*Rutherford Appleton Laboratory, Chilton, Didcot, Oxon, England*

⁽³⁾*Physics Department and Ames Laboratory, Iowa State University, Ames, Iowa 50011*

(Received 16 July 1992, revised manuscript received 30 September 1992)

Long-wavelength vacuum oscillations between neutrinos can explain all the existing results from the chlorine, water-Cherenkov, and new gallium solar neutrino detectors. They predict distinctive energy dependences and seasonal time dependences that can be measured in solar neutrino experiments currently being constructed.

PACS numbers: 96.60.Kx, 12.15.Ff, 14.60.Gh

The recent observation of solar neutrino signals in the ^{71}Ga detectors of the GALLEX and SAGE groups [1, 2] has added an important new constraint in the solar neutrino puzzle. GALLEX reports a signal of $83 \pm 19 \pm 5$ SNU (solar neutrino units) and SAGE reports $58^{+17}_{-24} \pm 14$ SNU to be compared with predictions of about 132 SNU in the standard solar model (SSM) [3, 4] with conventional neutrino propagation. This indicates a suppression ratio

$$R_{\text{Ga}}(\text{GALLEX}) = 0.63 \pm 0.16, \quad (1)$$

$$R_{\text{Ga}}(\text{SAGE}) = 0.44^{+0.17}_{-0.21},$$

relative to the latest Bahcall-Pinsonneault calculation [4], that differs from the corresponding suppression ratios

$$R_{\text{Cl}} = 0.26 \pm 0.05, \quad R_{\text{Kam II}} = 0.47 \pm 0.09, \quad (2)$$

in the classic ^{37}Cl Homestake detector [5] and in the water-Cherenkov (ν - e scattering) Kamiokande II detector [6], that have higher neutrino energy thresholds. Both experimental and theoretical uncertainties [4] are included here. The new solar neutrino puzzle is to explain these three different signals simultaneously.

A first discussion, presented by the GALLEX group [1] and amplified by others [7], argues that an explanation by nonstandard solar models is still conceivable though unpromising. They also show that explanations by matter-enhanced neutrino oscillations [the Mikheyev-Smirnov-Wolfenstein (MSW) effect [8]] are possible, for two distinct regions in the $(\sin^2 2\theta, \delta m^2)$ parameter plane. In-

deed, previous fits to the Homestake and Kamiokande II data already indicate where the new gallium results can be accommodated in a MSW scenario [9].

In the present Letter we point out an alternative explanation in terms of long-wavelength vacuum neutrino oscillations [10]; solutions of this kind [11–13], previously fitted to the Homestake and Kamiokande data, predict ^{71}Ga capture rates quite consistent with the new data. With such oscillations, having wavelengths comparable to the Earth-Sun distance, it is natural for some sections of the solar neutrino spectrum to be greatly suppressed while others suffer less suppression. In the following we shall first present updated long-wavelength oscillation (LWO) fits to the Homestake plus Kamiokande data, using the most recent version of the SSM [4] and incorporating the first 220 days' preliminary results from the upgraded Kamiokande III detector [14], that give

$$R_{\text{Kam III}} = 0.60^{+0.15}_{-0.13}. \quad (3)$$

Superposing these solutions on an iso-SNU plot of the corresponding predictions of a ^{71}Ga detector exhibits visually the range of gallium rates that is allowed for this kind of solution and the neutrino mass and mixing parameters that are required. Finally, we shall present LWO fits to the Homestake plus Kamiokande plus GALLEX and SAGE data simultaneously and discuss their predictions for future observations.

We have first refitted the LWO hypothesis to the latest suppression ratios from Homestake and Kamiokande III (above), together with the Kamiokande II ratios sepa-

rated into fourteen bins of recoil electron energy T_e [their weighted mean appears in Eq. (2)], in order to input the maximal pregalium spectral information. The initial solar neutrino spectrum is taken from the recent Bahcall-Pinsonneault [4] update of the SSM, that includes He diffusion and other improvements on previous calculations [3]. We assume two-flavor mixing of the electron neutrino ν_e , either with an active neutrino species ν_α ($\alpha = \mu$ or τ) or with a sterile neutrino ν_X ; these two scenarios are indistinguishable in ^{37}Cl or ^{71}Ga detectors, but give different results in detectors (including Kamiokande) that are sensitive to neutral-current scattering of ν_α . Figure 1 shows our resulting regions of fit in the $(\sin^2 2\theta, \delta m^2)$ plane, where θ is the usual mixing angle and δm^2 is the difference of mass-squared eigenvalues. There are sixteen data points (Cl rate, fourteen T_e bins from Kam II, Kam III rate) and two free parameters; the best fits give $\chi^2_{\min} = 12.5$ ($\nu_e-\nu_\alpha$) and 16.9 ($\nu_e-\nu_X$). The regions of fit have summed $\chi^2 < \chi^2_{\min} + 6.1$ corresponding to 95% C.L. Small discrepancies with some previous results [13] appear to be mainly due to small differences in data sets used. As in previous fits [9, 11, 13], sterile neutrino mixing solutions are more restricted but not excluded. We note that $\nu_e-\nu_X$ oscillations with maximal mixing are an essential feature of a recent custom-designed model [15] for the controversial 17 keV neutrino; in such models LWO are then preferable to MSW solutions as an explanation for the solar neutrino puzzle.

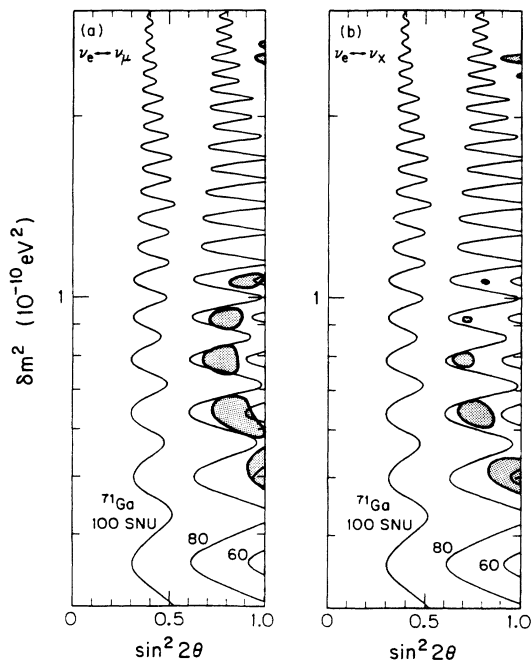


FIG. 1. LWO solutions to Homestake plus Kamiokande data are shown as shaded regions in the $(\sin^2 2\theta, \delta m^2)$ plane, for (a) $\nu_e-\nu_\alpha$ active neutrino mixing ($\alpha = \mu$ or τ) and (b) $\nu_e-\nu_X$ sterile neutrino mixing. Solid curves denote iso-SNU contours of the predicted ^{71}Ga capture rate in each case.

Figure 1 also shows time-averaged iso-SNU contours for the ^{71}Ga capture rate. The LWO regions of fit to Homestake and Kamiokande data fall almost entirely between the 60 SNU and 80 SNU contours, predicting ^{71}Ga capture rates compatible with the GALLEX and SAGE signals above (compatibility with preliminary SAGE data alone was previously discussed in Ref. [13]). This figure shows that the LWO hypothesis accommodates all the present gallium data quite naturally. It also shows where a future more precisely determined ^{71}Ga rate can fit in.

Finally we have fitted the LWO hypothesis to all Homestake plus Kamiokande plus both gallium results (eighteen data points with two free parameters); the best fit parameters are nearly identical to those in the fit without gallium data, giving $\chi^2_{\min} = 13.7$ for $\nu_e-\nu_\alpha$ oscillations and 18.7 for $\nu_e-\nu_X$ oscillations. Figure 2 shows the corresponding regions of fit at 95% C.L. in the $(\sin^2 2\theta, \delta m^2)$ plane. These regions summarize the LWO picture for present data.

The LWO predictions for future experiments are particularly sensitive to line sources in the solar neutrino spectrum, such as the 862-keV ^7Be line (that generates most of the wiggles in the ^{71}Ga contours in Fig. 1). Observations of ν - e scattering at the planned BOREXINO detector [16], in the electron recoil energy band $0.26 <$

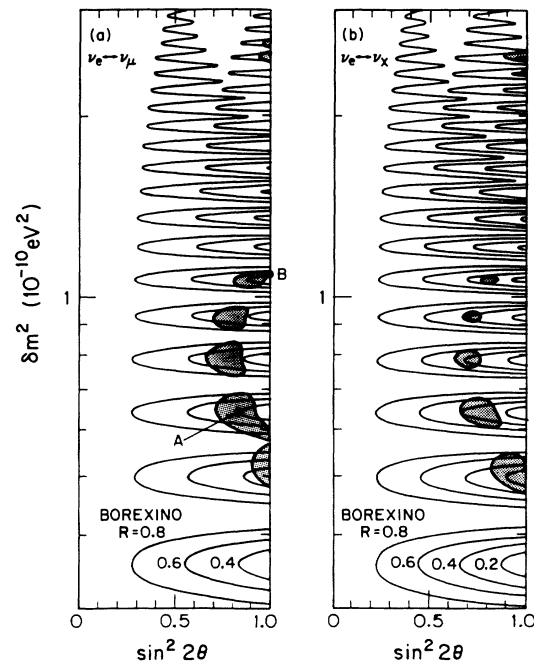


FIG. 2. LWO solutions to Homestake plus Kamiokande plus GALLEX plus SAGE data are shown as shaded regions in the $(\sin^2 2\theta, \delta m^2)$ plane, for (a) $\nu_e-\nu_\alpha$ mixing ($\alpha = \mu$ or τ) and (b) $\nu_e-\nu_X$ mixing. Solid curves are contours of the suppression ratio R for the time-averaged ν - e scattering signal in the BOREXINO detector, in the band $0.25 < T_e < 0.66$ keV. Points A and B are the two typical cases illustrated in Fig. 3.

$T_e < 0.66$ MeV, will be very sensitive to this ${}^7\text{Be}$ line contribution. Figure 2 shows contours of the time-averaged suppression factor R (BOREXINO) for this energy band; a range of possible values $0.3 \lesssim R \lesssim 0.9$ is allowed for ν_e - ν_α active neutrino oscillations, or $0.1 \lesssim R \lesssim 0.4$ for ν_e - ν_X sterile neutrino oscillations. These fully overlap the range 0.21–0.65 expected for MSW solutions [7, 9]; unless the BOREXINO results lie outside the MSW band, or future data make the bands much narrower, this time-averaged measurement alone will not discriminate sharply between MSW and LWO solutions. One may also look at higher T_e bands, containing pep , ${}^{13}\text{N}$, and ${}^{15}\text{O}$ neutrinos, but here the event rate is much lower.

A distinctive feature of LWO scenarios, however, is that they contain clean and potentially resolvable oscillations in the ν_e survival probability $P(\nu_e \rightarrow \nu_e) = 1 - \sin^2 2\theta \sin^2(\delta m^2 L/4E)$, where L is the distance from source to detector. This feature is absent in MSW scenarios with larger δm^2 values where the corresponding oscillatory factors are averaged due to the size of the solar source and the detector energy resolution [17]. An immediate consequence is a time dependence of the contributions from line sources, due to the seasonal changes in the Earth-Sun distance [10–13]; here we fix E and find L dependence in $P(\nu_e \rightarrow \nu_e)$. Eventually, it should be possible to discriminate between LWO and other explanations on this basis alone, but at present there is little evidence on this score. The ${}^{37}\text{Cl}$ capture rate has a ${}^7\text{Be}$ component and could exhibit some time dependence; it is intriguing to find that our best fit with LWO to the seasonal ${}^{37}\text{Cl}$ data (cited in Ref. [18]) is actually better (lower χ^2) than a fit to constant R_{Cl} , although with little statistical significance at present. The ${}^{71}\text{Ga}$ and BOREXINO signals, however, contain larger ${}^7\text{Be}$ components and could provide better evidence (already discussed in Refs. [9, 11–13]). Typical LWO solutions with δm^2 of order 5×10^{-11} , 1×10^{-10} , and 2.5×10^{-10} eV² have differences between maximal and minimal six-month ${}^{71}\text{Ga}$ count rate of up to 8, 17, and 29 SNU, respectively, due to the variation in the Earth-Sun distance. Ultimately, the statistical uncertainty in a six-month gallium measurement may be reduced to 7 SNU, so these variations may be detectable in ${}^{71}\text{Ga}$ for solutions with larger δm^2 . In the BOREXINO experiment the count rate is much higher; the statistical uncertainty in the monthly measurement of R may be as low as 0.04. The differences between maximal and minimal monthly measurements of R in BOREXINO cover the ranges 0.02–0.24, 0.09–0.45, and 0.39–0.66, respectively, for LWO solutions in the three aforementioned δm^2 regions. Hence, there is a strong likelihood that the LWO time dependence could be observed in BOREXINO. A statistical analysis of the time dependence of BOREXINO counting rates, divided into four energy regions that approximately separate the ${}^7\text{Be}$, pep , and CNO contributions, indicates that one year's running (about 20 000 events) could distinguish

all our LWO solutions from time-independent MSW solutions; it would also distinguish most of our LWO solutions from each other.

The Sudbury Neutrino Observatory (SNO) [19] cannot detect ${}^7\text{Be}$ neutrinos and will see little time dependence, but will be able to test a second distinctive property of LWO, namely, an oscillatory modulation of the ${}^8\text{B}$ neutrino spectrum. This property follows immediately from the expression for $P(\nu_e \rightarrow \nu_e)$, that oscillates versus E_ν when measured at (approximately) constant L . SNO will determine the high-energy ${}^8\text{B}$ neutrino spectrum through its measurement of charged-current (CC) $\nu_e d \rightarrow ppe^-$ scattering. Here the electron energy is closely correlated with the incident neutrino energy, peaking at $E_e = E_\nu - 1.4$ MeV, so that the neutrino spectrum will be measured directly, not averaged (as in ${}^{37}\text{Cl}$ capture) nor strongly smeared by the recoil electron distribution (as in ν - e scattering). $P(\nu_e \rightarrow \nu_e)$ is given by the ratio of the observed neutrino spectrum to the calculated ${}^8\text{B}$ spectrum; the normalization of the latter may be affected by the solar model but the shape is not. Figure 3 illustrates the dependence of $P(\nu_e \rightarrow \nu_e)$ on E_ν for two typical LWO solutions, labeled A and B in Fig. 2 (including an average over the varying Earth-Sun distance); we see distinctive oscillations in the LWO cases as E_ν decreases. SNO is expected to extract a solar signal at least for $E_e > 5$ MeV ($E_\nu \gtrsim 6.4$ MeV); it may, however, be possible to push the threshold down toward $E_e > 4$ MeV ($E_\nu \gtrsim 5.4$ MeV) to obtain better discrimination between different cases. Statistical analysis of the E_e spectrum shape alone, based on 6000 CC events with $E_e > 5$ MeV (from two years running) indicates

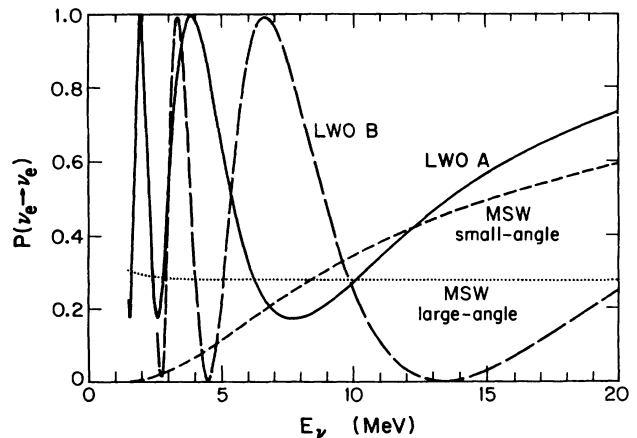


FIG. 3. Electron-neutrino survival probability $P(\nu_e \rightarrow \nu_e)$ is shown vs neutrino energy E_ν for two typical LWO solutions A ($\delta m^2 = 6.4 \times 10^{-11}$ eV², $\sin^2 2\theta = 0.83$, solid curve) and B ($\delta m^2 = 1.1 \times 10^{-10}$ eV², $\sin^2 2\theta = 1.00$, long-dashed curve). We also show solutions typifying the two MSW regions of fit: $\delta m^2 = 5.0 \times 10^{-6}$ eV², $\sin^2 2\theta = 0.008$ (short-dashed curve) and $\delta m^2 = 1.0 \times 10^{-5}$ eV², $\sin^2 2\theta = 0.8$ (dotted curve).

that almost all our LWO solutions would be distinguishable from MSW, but a small region near LWO A would be confused with small-angle MSW; with $E_e > 4$ MeV, however, all our LWO solution regions would be clearly distinguishable from MSW. This analysis includes both the dynamical spread in the E_e spectrum and the experimental resolution. If this ^8B spectrum modulation or the ^7Be time dependence were detected, it would provide the first case(s) in which a resolved neutrino oscillation had been seen.

SNO will also detect neutral-current (NC) $\nu_\alpha d \rightarrow \nu_\alpha pn$ scattering, which will determine if oscillations are occurring to sterile neutrinos. In a sterile neutrino oscillation scenario both CC and NC rates would be suppressed (to perhaps $R \approx 0.4$), while for ν_e - ν_α oscillations only CC would be suppressed.

We conclude the following.

(a) The LWO hypothesis with two-neutrino mixing can comfortably account for the present ^{37}Cl , Kamiokande, and ^{71}Ga data. There are discrete regions of fit as shown, for either active or sterile neutrino mixing.

(b) Time-averaged BOREXINO measurements may not cleanly discriminate between LWO and MSW solutions, since their predictions overlap considerably.

(c) A distinctive signature of LWO solutions, however, is the seasonal time dependence of the ^7Be line. There is at present just a hint in the ^{37}Cl data, but future BOREXINO measurements could probably detect this seasonal dependence, discriminating all LWO solutions from MSW solutions and most LWO solutions from each other.

(d) Another distinctive LWO signature is the oscillatory modulation of the ^8B spectrum shape. Future SNO data should discriminate all (or almost all) LWO solutions from MSW in this way, depending on the E_e detection threshold.

(e) Measurements of NC scattering in SNO would discriminate between active neutrino and sterile neutrino mixing options. More precise data of all kinds should also restrict the options in the future.

We have discussed mixing between two neutrino species, but three-neutrino mixing is another possibility. Although the maximal three-neutrino mixing case (which predicts $R_{\text{Kam}} = 0.43$ and a ^{71}Ga rate of 44 SNU) is clearly disfavored by the new Kamiokande III and GALLEX data, many other scenarios with mass-squared difference scales in the $\delta m^2 \sim 10^{-10}$ eV² range can comfortably account for these results [9, 11, 12]. The allowed range of BOREXINO predictions is larger, and the three-neutrino solutions have the characteristic seasonal variations and oscillatory modulation of two-neutrino LWO.

We thank David Wark for discussions about SNO. One of us (V.B.) thanks the Aspen Center for Physics for hospitality during the completion of this work. This research was supported in part by the U.S. Department of Energy under Contracts No. DE-AC02-76ER00881 and No. W-

7405-Eng-82, Office of Energy Research (KA-01-01), Division of High Energy and Nuclear Physics, and in part by the University of Wisconsin Research Committee with funds granted by the Wisconsin Alumni Research Foundation.

- [1] GALLEX Collaboration, P. Anselmann *et al.*, Phys. Lett. B **285**, 376 (1992); **285**, 390 (1992).
- [2] SAGE Collaboration, A. I. Abazov *et al.*, Phys. Rev. Lett. **67**, 3332 (1991); A. Garvin, in Proceedings of the Twenty-Sixth International Conference on High Energy Physics, Dallas, August 1992 (to be published).
- [3] For a review, see J. N. Bahcall and R. K. Ulrich, Rev. Mod. Phys. **60**, 297 (1988).
- [4] J. N. Bahcall and M. H. Pinsonneault, Princeton Report No. IASSNS-AST 92/10 (to be published).
- [5] R. Davis, Jr., in *Proceedings of Thirteenth Conference on Neutrino Physics and Astrophysics, Boston, 1988*, edited by J. Schneps *et al.* (World Scientific, Singapore, 1989), p. 518.
- [6] K. S. Hirata *et al.*, Phys. Rev. D **44**, 2241 (1991).
- [7] J. M. Gelb, W. Kwong, and S. P. Rosen, Phys. Rev. Lett. **69**, 1864 (1992); S. A. Bludman, N. Hata, D. C. Kennedy, and P. G. Langacker, University of Pennsylvania Report No. UPR-0516T (unpublished).
- [8] S. P. Mikheyev and A. Yu. Smirnov, Yad. Fiz. **42**, 1441 (1985) [Sov. J. Nucl. Phys. **42**, 913 (1985)]; Nuovo Cimento Soc. Ital. Fis. **9C**, 17 (1986); L. Wolfenstein, Phys. Rev. D **17**, 2369 (1978); **20**, 2634 (1979).
- [9] V. Barger, R. J. N. Phillips, and K. Whisnant, Phys. Rev. D **43**, 1110 (1991); T. K. Kuo and J. Pantaleone, Phys. Rev. D **41**, 3842 (1990); Mod. Phys. Lett. A **6**, 15 (1991); V. Barger, N. Deshpande, P. B. Pal, R. J. N. Phillips, and K. Whisnant, Phys. Rev. D **43**, 1759 (1991).
- [10] V. Gribov and B. Pontecorvo, Phys. Lett. **28B**, 493 (1969); S. M. Bilenky and B. Pontecorvo, Phys. Rep. **41**, 225 (1978); V. Barger, R. J. N. Phillips, and K. Whisnant, Phys. Rev. D **24**, 538 (1981); S. L. Glashow and L. M. Krauss, Phys. Lett. B **190**, 199 (1987).
- [11] V. Barger, R. J. N. Phillips, and K. Whisnant, Phys. Rev. Lett. **65**, 3084 (1990).
- [12] A. Acker, S. Pakvasa, and J. Pantaleone, Phys. Rev. D **43**, 1754 (1991).
- [13] P. I. Krastev and S. T. Petcov, Phys. Lett. B **285**, 85 (1992).
- [14] K. Nakamura, in Proceedings of the Neutrino '92 Conference, Granada, June 1992 (to be published).
- [15] E. Ma, Phys. Rev. Lett. **68**, 1981 (1992).
- [16] R. S. Raghaven, in *Proceedings of the Twenty-Fifth International Conference on High Energy Physics, Singapore, 1990*, edited by K. K. Phua and Y. Yamaguchi (World Scientific, Singapore, 1991).
- [17] J. N. Bahcall and S. C. Frautschi, Phys. Lett. **29B**, 623 (1969).
- [18] M. Cribier *et al.*, Phys. Lett. B **188**, 168 (1987).
- [19] G. T. Ewan *et al.*, Sudbury Neutrino Observatory Proposal No. SNO-87-12, 1987.

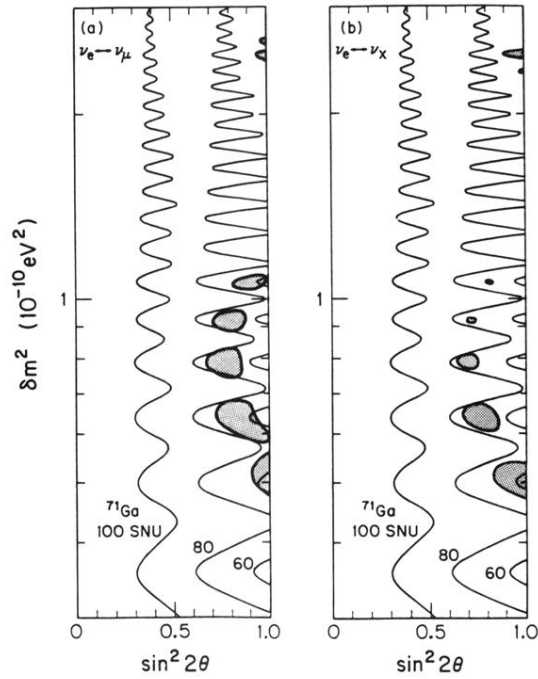


FIG. 1. LWO solutions to Homestake plus Kamiokande data are shown as shaded regions in the $(\sin^2 2\theta, \delta m^2)$ plane, for (a) $\nu_e - \nu_\alpha$ active neutrino mixing ($\alpha = \mu$ or τ) and (b) $\nu_e - \nu_\chi$ sterile neutrino mixing. Solid curves denote iso-SNU contours of the predicted ^{71}Ga capture rate in each case.

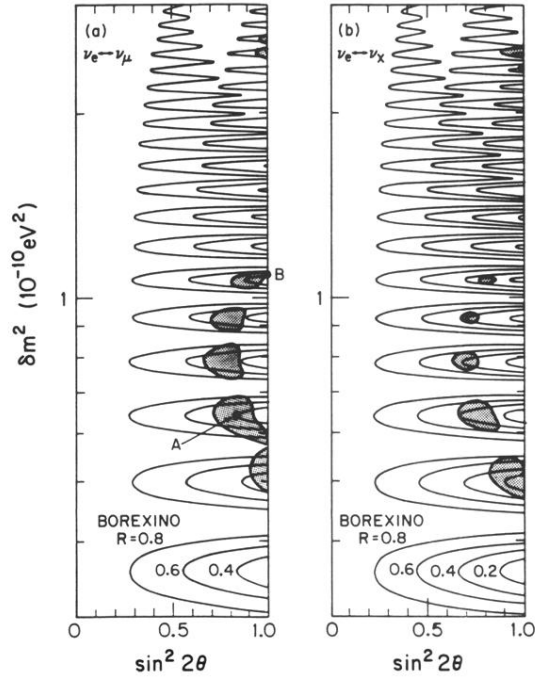


FIG. 2. LWO solutions to Homestake plus Kamiokande plus GALLEX plus SAGE data are shown as shaded regions in the $(\sin^2 2\theta, \delta m^2)$ plane, for (a) $\nu_e-\nu_\alpha$ mixing ($\alpha = \mu$ or τ) and (b) $\nu_e-\nu_X$ mixing. Solid curves are contours of the suppression ratio R for the time-averaged ν - e scattering signal in the BOREXINO detector, in the band $0.25 < T_e < 0.66$ keV. Points A and B are the two typical cases illustrated in Fig. 3.